Inclusion of Carrier-Carrier-Scattering Into Arbitrary-Order Spherical Harmonics Expansions of the Boltzmann Transport Equation

K. Rupp*†, P.W. Lagger*, and T. Grasser*
*Institute for Microelectronics, TU Wien, Gußhausstraße 27–29/E360, A-1040 Wien, Austria
†Institute for Analysis and Scientific Computing, TU Wien, Wiedner Hauptstraße 8–10/E101, A-1040 Wien, Austria

INTRODUCTION

The deterministic Spherical Harmonics Expansion (SHE) method for the numerical solution of the Boltzmann Transport Equation (BTE) has become an attractive alternative to the stochastic Monte-Carlo (MC) method. While the method has long been limited to one-dimensional device simulation due to memory constraints, modern workstations provide enough resources for running two- and even three-dimensional simulations [1], [2]. Also, excellent agreement with MC results became only possible after the method had been extended to arbitrary expansion orders [3]. However, despite the availability of a suitable formalism for a wide range of common scattering operators, the inclusion of carrier-carrier scattering (cc-scattering) has only been considered in a very early publication for first-order SHE [4]. In this work we present a methodology for the inclusion of carrier-carrier scattering into arbitrary-order SHE and discuss the implications on the computational effort as well as the memory requirements.

CARRIER-CARRIER SCATTERING FOR SHE

Using a low-density approximation and neglecting the Pauli-principle, most scattering mechanisms lead to a linear scattering operator. However, cc-scattering leads to a quadratic scattering operator of the form

$$Q_{\mathrm{cc}}\{f\} = \int s(\boldsymbol{k}',\boldsymbol{k},\boldsymbol{k}_2',\boldsymbol{k}_2) f(\boldsymbol{k}') f(\boldsymbol{k}_2') - s(\boldsymbol{k},\boldsymbol{k}',\boldsymbol{k}_2,\boldsymbol{k}_2') f(\boldsymbol{k}) f(\boldsymbol{k}_2) \,\mathrm{d}(\boldsymbol{k}',\boldsymbol{k}_2,\boldsymbol{k}_2') \ ,$$

where f is the carrier distribution function, $\boldsymbol{k}$, $\boldsymbol{k}_2$, $\boldsymbol{k}'$, $\boldsymbol{k}_2'$ are the wave vectors, and $s = \sigma_{\mathrm{cc}}\delta(\varepsilon+\varepsilon'-\varepsilon_2-\varepsilon_2')$. The coefficient σ_{cc} is proportional to

$$\sigma_{\mathrm{cc}}(\boldsymbol{k},\boldsymbol{k}',\boldsymbol{k}_2,\boldsymbol{k}_2') \simeq \frac{n\delta(\boldsymbol{k}+\boldsymbol{k}'-\boldsymbol{k}_2-\boldsymbol{k}_2')}{\left[(\boldsymbol{k}-\boldsymbol{k}')+1/\lambda_{\mathrm{D}}^2\right]^2}$$

and includes the carrier density n, the Debye-length λ_{D}, a delta distribution for the conservation of momentum, and shows a strong angular dependence. Since the denominator is identical to that from ionized impurity scattering, we treat it in the same way using an isotropic approximation with identical momentum relaxation times [5]. This allows for the derivation of an expression for the projected scattering operator onto the spherical harmonic $Y_{l,m}$ as

$$Q_{\mathrm{cc};l,m}\{f\} = \frac{Z}{Y_{0,0}^3}\int_0^\infty \sigma_{\mathrm{cc}}\big[f_{0,0}(\varepsilon')f_{0,0}(\varepsilon+\varepsilon^*-\varepsilon') - f_{0,0}(\varepsilon^*)f_{l,m}(\varepsilon)\big] \times Z(\varepsilon')Z(\varepsilon+\varepsilon^*-\varepsilon')\,\mathrm{d}\varepsilon' \ .$$

Here, Z is the density of states and ε^* denotes the energy of the second carrier. Since this second energy is unknown by nature, we propose a weighted average over all energies. As a computationally cheaper alternative, one may also set ε^* to the average carrier energy at the respective location inside the device at the price of possibly reduced accuracy. Note that the scattering operator vanishes for the case of f being given by a Maxwell distribution and is thus consistent with other scattering mechanisms.

RESULTS

The proposed model is implemented in our free open source simulator ViennaSHE [6] and evaluated for bulk silicon in Fig. 1 and Fig. 2. It is shown that our method is able to resolve the high energy tails of the distribution function well. Only a few additional nonlinear Picard iterations are sufficient for convergence. In Fig. 3 our method is applied to two MOSFET devices with different channel lengths. An elevation of the high-energy tail due to cc-scattering is observed, emphasizing the importance of cc-scattering for predictive device simulation. The drawback of the proposed method is that the integral expression for $Q_{\mathrm{cc};l,m}$ couples all energies with each other, which leads to a quadratic dependence of the computational effort on the number of energy points, cf. Fig. 4.

CONCLUSION

We have suggested a formulation that allows for the inclusion of cc-scattering into arbitrary-order SHE. An initial comparison shows good agreement with bulk MC results and can also be used on two or three-dimensional geometries.

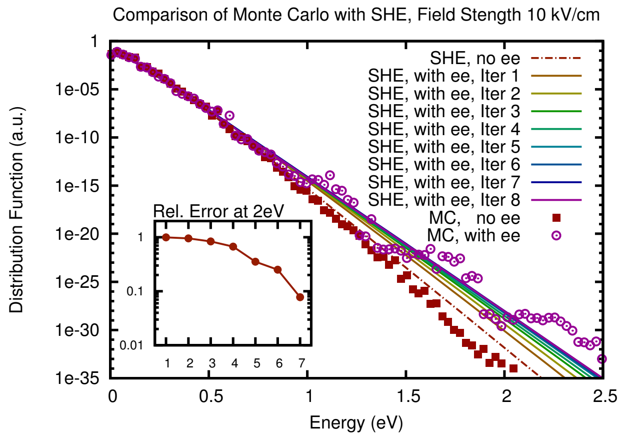

Fig. 1. Simulation of the electron distribution with and without electron-electron (ee) scattering in bulk silicon at an applied field of 10 kV/cm. The elevation of the distribution function at higher energies is well reflected by SHE with the proposed method. After at most eight Picard iterations, the change of the distribution function becomes negligible.

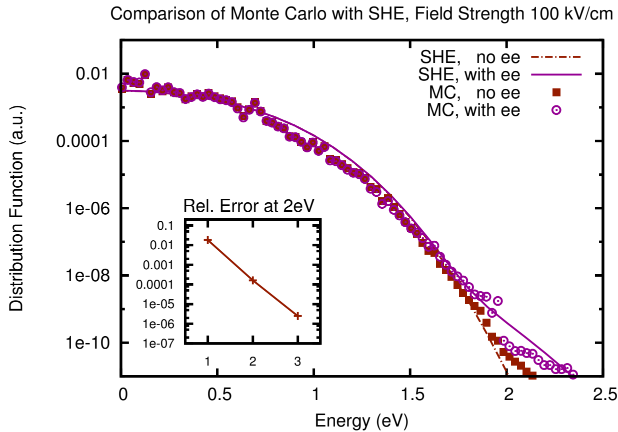

Fig. 2. Simulation of the electron distribution with and without ee-scattering in bulk silicon at an applied field of 100 kV/cm. The high-energy tail of the distribution function around 2 eV is essentially resolved by the proposed method after only one Picard iteration.

REFERENCES

[1] S.-M. Hong *et al*, *Deterministic Solvers for the Boltzmann Transport Equation*. Springer, 2011.

[2] K. Rupp *et al.*, On the Feasibility of Spherical Harmonics Expansions of the Boltzmann Transport Equation for Three-Dimensional Device Geometries. *IEDM Techn. Digest*, 2011.

[3] C. Jungemann *et al.*, Stable Discretization of the Boltzmann Equation based on Spherical Harmonics, Box Integration, and a Maximum Entropy Dissipation Principle. *J. Appl. Phys.*, 2006.

[4] A. Ventura *et al.*, Inclusion of Electron-Electron Scattering in the Spherical Harmonics Expansion Treatment of the Boltzmann Transport Equation. *Proc. SISDEP*, 1993.

[5] C. Jungemann and B. Meinerzhagen. *Hierarchical Device Simulation*. Springer, 2003.

[6] ViennaSHE. `http://viennashe.sourceforge.net/`

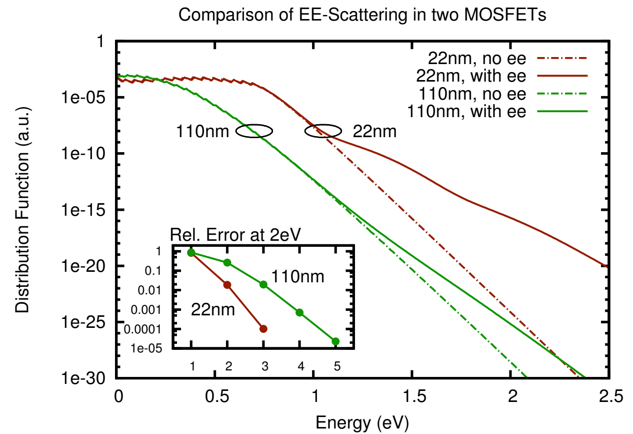

Fig. 3. Comparison of the electron energy distribution function at channel-drain transition region for a 22nm and a 110nm MOSFET device with $V_{\mathrm{DS}} = 1.0$ Volt and $V_{\mathrm{G}} = 0.8$ Volt. The influence of cc-scattering on the high-energy tail of the distribution function is particularly pronounced in the smaller device. After at most three Picard iterations, convergence for practical purposes is obtained. The ripples at lower energies are due to optical phonon scattering.

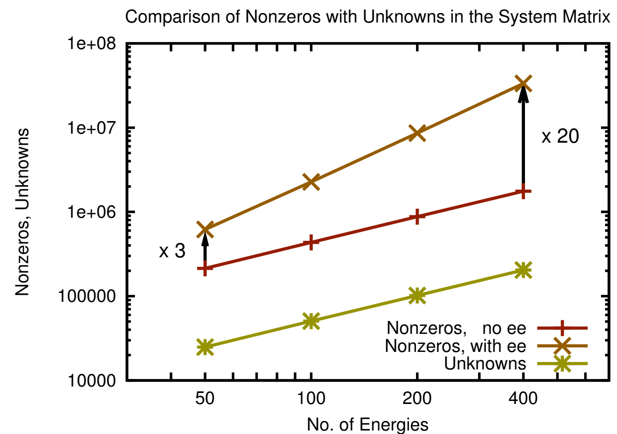

Fig. 4. Nonzeros and number of unknowns of the system matrix for a 22nm MOSFET device. While both the number of unknowns and the number of nonzeros in the system matrix scale linearly with the number of energy points, carrier-carrier scattering leads to a coupling of all energy points, leading to quadratic effort. Memory requirements and simulation times are consequently increased by a factor of three using 50 energy points and up to a factor of 20 when using 400 points in total energy direction. With typically 100 to 200 energy points per electron volt, one thus has to expect increased memory requirements of one order of magnitude in low-voltage applications.

ACKNOWLEDGEMENTS

The authors wish to thank P. Palestri and A. Zaka for providing Monte Carlo data for comparison. K. Rupp gratefully acknowledges support by the Graduate School PDETech at the TU Wien. K. Rupp and T. Grasser acknowledge support by the Austrian Science Fund (FWF), grant P23598.